Actively *Q*-switched ring Tm-doped fiber laser with free space structure

Wei Liu (刘 伟), Youlun Ju (鞠有伦)*, Tongyu Dai (戴通宇), Liwei Xu (徐丽伟), Jinhe Yuan (袁晋鹤), Chao Yang (杨 超), Baoquan Yao (姚宝权), and Xiaoming Duan (段小明)

National Key Laboratory of Tunable Laser Technology, Harbin Institute of Technology, Harbin 150001, China

**Corresponding author: juyoulun@126.com*

Received April 25, 2016; accepted June 24, 2016; posted online July 20, 2016

We report a cladding-pumped actively *Q*-switched ring Tm-doped fiber laser (TDFL). This laser is *Q*-switched by a free space acousto-optic modulator. A pulse energy up to 150 μJ with a pulse width of 207 ns at a repetition rate of 100 Hz is achieved for a cavity optical length of 6.68 m. The pulse amplitude's stability at this repetition rate is better than 95%. To the best of our knowledge, this is the first free space structure *Q*-switched ring TDFL report.

OCIS codes: 140.3480, 140.3510, 140.3538, 140.3540.
doi: 10.3788/COL201614.091401.

In recent years, pulsed lasers emitting at wavelengths in the 2 μm region have attracted a lot of interest for many applications such as remote sensing, LIDAR systems, and pump sources for optical parametric oscillators[1–3]. Benefitting from the characteristics of good beam quality, broad spectral emission, compact assembly, and high efficiency[4,5], a Tm-doped fiber laser (TDFL) plays an important role among 2 μm lasers. For Doppler LIDAR wind sensing systems the emission source with a proper long pulse width is beneficial to measurement accuracy[6]. A pulsed fiber ring laser is usually used as a slave laser to be injected by a seed laser, which is an important component of the emission source for a LIDAR (or remote sensing) system[7,8]. Due to a low cavity loss, the pulse width of a fiber ring laser could be broadened by increasing the fiber length[9].

In 2012, Jung *et al.* reported a passive *Q*-switched ring TDFL based on carbon nanotube evanescent field interaction, with a temporal pulse width of ~7.155 μs[10]. In 2014, Ahmad *et al.* demonstrated a passive pulsed ring TDFL by using multiwalled carbon nanotubes embedded in polyvinyl alcohol as the saturable absorber[11]. The laser has a pulse width of 7.93 μs and a pulse energy of 103.37 nJ. Passively *Q*-switched lasers have simple structures, but the repetition rate and pulse width are usually uncontrolled. In contrast, active *Q*-switching technology could provide more control over the characteristics of output pulses[12]. An acousto-optic modulator (AOM) is a conventional choice for active *Q*-switching due to the characteristics of fast switching speed, low modulation voltage, and stable repetition frequency. Presently, there are two types of AOMs: fiber coupled and free space. Generally speaking, a free space AOM has a higher damage threshold than a fiber-coupled AOM in the 2 μm region. In 2015, Gutty *et al.* reported a core-pumped TDFL by employing a free space AOM[13]. A peak power up to 7 kW with a repetition rate of 1 kHz was achieved.

In this Letter, we present an actively *Q*-switched ring TDFL with a free space structure. The laser produced a pulse energy of 150 μJ at a repetition rate of 100 Hz with a pulse width of 207 ns. Then the cavity optical length was increased to 12 m by adding a passive fiber; meanwhile, a pulse width of 382 ns with an output pulse energy of 150 μJ was achieved. We expect that the actively *Q*-switched ring TDFL will provide a proper pulse width for a Doppler LIDAR system.

The experimental setup used for the ring TDFL is shown in Fig. 1. The pump sources for the TDFL are two 50 W fiber-coupled pump diodes (200/220 0.22 NA delivery fiber) with a $(2+1)\times 1$ combiner to provide about 100 W of 790 nm pump power. The active fiber has a core diameter of 25 μm/0.10 NA, a 400 μm cladding, and an absorption coefficient of ~1.67 dB/m at 790 nm. The 2 m-long active fiber is wrapped around a 15 cm diameter aluminum mandrel water-cooled at 15°C. The total length of the laser cavity is 6.68 m. At the output end of the fiber an end cap coated for high transmission at the laser wavelength is employed. The end cap could avoid the parasitic oscillation caused by fiber-facet reflection and ensure that the signal intensity is well below the surface damage threshold for facets of the fiber ends.

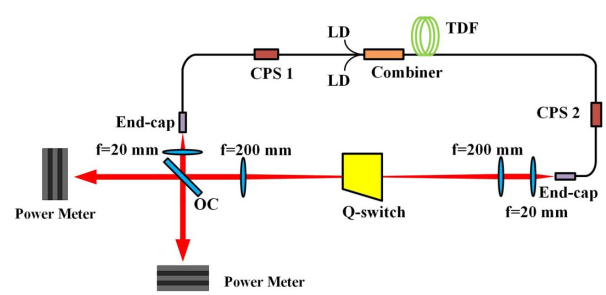

Fig. 1. *Q*-switched ring TDFL schematic.

The output coupler (OC) is a flat mirror coated with 90% reflectivity at 2 μm.

An AOM is used to switch the quality factor of the laser at a 100 Hz repetition rate. Both surfaces of the AOM are coated with high transmission layer of around 2 μm. The active aperture of the AOM is 1 mm. Two lenses are used to reshape the beam of the laser to keep in accordance with the active aperture of the AOM. Light from the end cap of the fiber is collimated by a plane convex lens with a 20 mm focal length, and then focused by a lens with a focal length of 200 mm. The coupling efficiency of the lenses to fiber was measured to be about 50%. All the lenses are coated with a high transmission layer of around 2 μm. Generally, the light traveling in the cladding consists of amplified spontaneous emission (ASE), the residual pump light, and the core light leaking into the cladding. The ASE will form the multipeak structure in the output pulse for the Q-switched laser[14]. The residual pump light and the signal light in the cladding have a strong effect on the quality of the laser system and the output beam. Two cladding power strippers (CPS) are employed to strip most of these unwanted lights, although this will lower the slope efficiency of the fiber ring TDFL laser.

First, the output pulse energy of the TDFL was investigated. The value for the energy per pulse was obtained by dividing the average output power by the repetition rates. The average output power was a total power consisting of two output directions which was measured by a power meter (LPE-1 A) with a resolution limited to 0.1 mW. The acoustic mode of the AOM used in the experiment is compressional, so it had a low diffraction efficiency for fiber lasers. The diffraction efficiency of the AOM was approximately 45%. The TDFL could not switch off completely when the pump power was over 24.4 W, which made us fail to achieve a higher output energy. Figure 2 shows the energy per pulse of the Q-switched fiber laser with respect to the pump power. The energy increased with the pump power. The TDFL had a threshold pump power of 20 W, and the maximum energy of 150 μJ at a repetition of 100 Hz was obtained under the pump power of 24.4 W. The output pulse energy curve showed a severe deviation from linearity that was properly due to the ASE in the fiber laser.

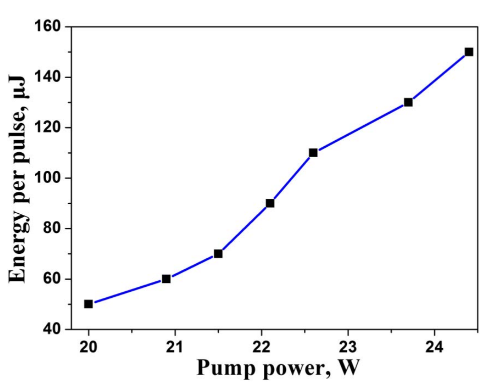

Fig. 2. Pulse energy as a function of pump power at 100 Hz.

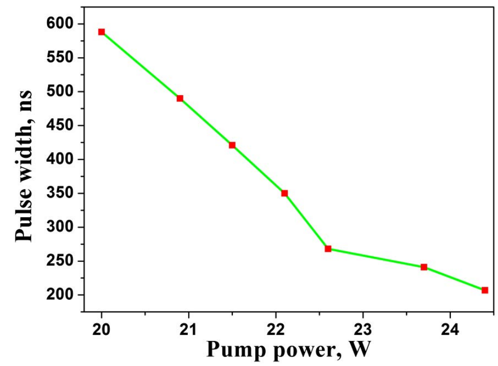

Fig. 3. Pulse width as a function of pump power for a cavity length of 6.68 m.

At a constant repetition rate of 100 Hz, the pulse width narrowing characteristic with pump power is shown in Fig. 3. The pulse width was obviously reduced with increasing pump power. A pulse width of 207 ns with a pulse energy of 150 μJ was achieved. The typical train of the stable pulse and the corresponding single pulse profile recorded under the pump power of 24.4 W are shown in Fig. 4. The train of actively Q-switched pulses had the same pulse repetition rate with the modulation frequency, and the stability of the pulse amplitude was better than 95%. The pulse shape showed a few multiple peaks, which resulted from the mode beating in the fiber laser[15].

For Q-switched fiber lasers, the pulse width could be modulated by changing the cavity optical length. Then the cavity length was increased to 12 m by adding a passive fiber into the laser cavity. As seen from Fig. 5, the pulse width increased significantly for a cavity length of 12 m compared with the cavity length of 6.68 m. The shortest pulse width of the ring TDFL with a cavity length of 12 m was about 382 ns.

The output spectra of the Q-switched TDFL running at 100 Hz were measured with the output pulse energy of 70 and 150 μJ, respectively. The spectra were recorded by a

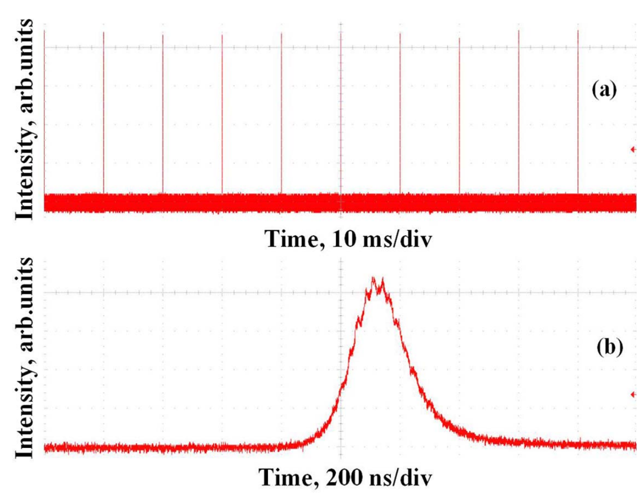

Fig. 4. Typical train of pulses and pulse shape at a repetition rate of 100 Hz: (a) a pulse train and (b) a single pulse.

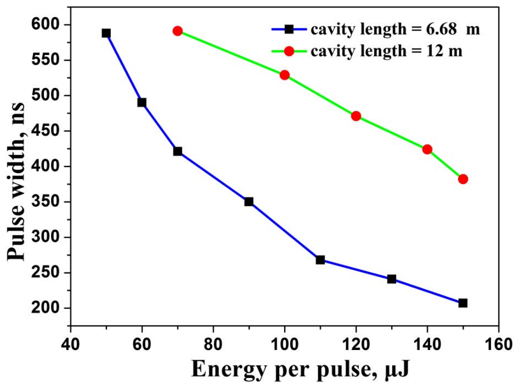

Fig. 5. Pulse width of the TDFL for different cavity lengths as a function of the output pulse energy.

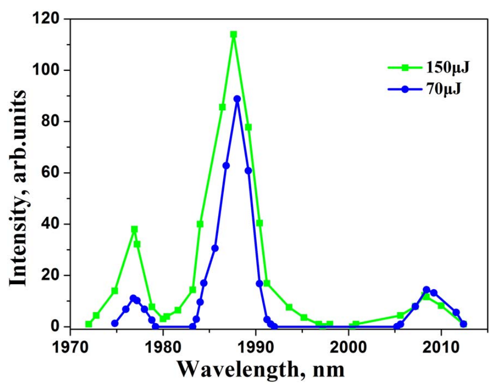

Fig. 6. Typical spectra of the output laser at 70 and 150 μJ, respectively.

WDG30-Z grating monochromator and a Tektronix digital oscilloscope (300 MHz) with an InGaAs detector. As shown in Fig. 6, the TDFL has three main emission peaks at 1977, 1988, and 2008 nm. The presence of multiple wavelengths was probably due to the broad emission spectra of the Tm-doped fiber and a relative low pump power leading to a weak mode competition. As the output pulse energy increased from 70 to 150 μJ the spectra shifted slightly and broadened obviously via Raman self-frequency shift[16].

In conclusion, we demonstrate the performance of a *Q*-switched ring TDFL with free space structure. This ring TDFL can generate pulses with a stable repetition rate and a proper long width for a Doppler LIDAR system, meanwhile the ring TDFL also requires fine alignment and good mechanical stability. The maximum pulse energy is 150 μJ with a 207 ns pulse width at a 100 Hz repetition rate for the cavity optical length of 6.68 m. For the same pulse energy output, the pulse width of 382 ns is obtained by increasing the cavity optical length of the ring TDFL to 12 m. Due to low diffraction efficiency of the AOM, a higher pulse energy output of the ring TDFL is not obtained.

This work was supported by the National Natural Science Foundation of China (Nos. 61308009, 61405047, and 51572053), the Fundamental Research Funds for the Central Universities (Nos. HIT.NSRIF.2014044 and HIT.NSRIF.2015042), the Science Fund for Outstanding Youths of Heilongjiang Province (No. JQ201310), and the China Postdoctoral Science Foundation (No. 2015T80339).

References

1. J. B. Barria, D. Mammez, E. Cadiou, J. B. Dherbecourt, M. Raybaut, T. Schmid, A. Bresson, J. M. Melkonian, A. Godard, J. Pelon, and M. Lefebvre, Opt. Lett. **39**, 6719 (2014).
2. C. T. Wu, F. Chen, and Y. L. Ju, J. Russ. Laser Res. **35**, 347 (2014).
3. E. Ji, Q. Liu, Z. Hu, P. Yan, and M. Gong, Chin. Opt. Lett. **12**, 121402 (2015).
4. J. Q. Xu, J. R. Lu, M. Prabhu, and K. Ueda, Proc. Soc. Photo-Opt. Instrum. Eng. **4270**, 88 (2001).
5. Y. Wang, J. L. Yang, C. Y. Huang, Y. F. Luo, S. W. Wang, Y. L. Tang, and J. Q. Xu, Opt. Express **23**, 2991 (2015).
6. T. Y. Dai, Y. L. Ju, X. M. Duan, Y. J. Shen, B. Q. Yao, and Y. Z. Wang, Appl. Phys. Express **5**, 082702 (2012).
7. R. J. Zhou, W. Shi, E. Petersen, A. Chavez-Pirson, M. Stephen, and N. Peyghambarian, J. Lightwave Technol. **30**, 2589 (2012).
8. P. D. Dragic, IEEE Photon. Technol. Lett. **16**, 1822 (2004).
9. T. Liu, D. Jia, Y. Liu, Z. Wang, and T. Yang, Chin. Opt. Lett. **10**, 101401 (2015).
10. M. Jung, J. Koo, Y. M. Chang, P. Debnath, Y. W. Song, and J. H. Lee, Laser Phys. Lett. **9**, 669 (2012).
11. M. T. Ahmad, A. A. Latiff, Z. Zakaria, D. I. M. Zen, N. Saidin, H. Haris, H. Ahmad, and S. W. Harun, Microwave Opt. Technol. Lett. **56**, 2817 (2014).
12. Z. W. Yu, M. Malmstrom, O. Tarasenko, W. Margulis, and F. Laurell, Opt. Express **18**, 11052 (2010).
13. F. Gutty, A. Grisard, A. Joly, C. Larat, D. Papillon-Ruggeri, and E. Lallier, Opt. Express **23**, 6754 (2015).
14. Q. Sun, Q. H. Mao, X. D. Chen, S. J. Feng, W. Q. Liu, and J. W. Y. Lit, Laser Phys. **20**, 1438 (2010).
15. P. Myslinski, J. Chrostowski, J. A. K. Koningstein, and J. R. Simpson, Appl. Opt. **32**, 286 (1993).
16. V. Philippov, J. K. Sahu, C. Codemard, W. A. Clarkson, J. N. Jang, J. Nilsson, and G. N. Pearson, Proc. Soc. Photo-Opt. Instrum. Eng. **5335**, 1 (2004).